Numerical modelling of deep coaxial borehole heat exchangers in the Cheshire Basin, UK

Christopher S. Brown[1*], Nigel J. Cassidy[1], Stuart S. Egan[2], Dan Griffiths[3]

Manuscript written for the Journal Computers and Geoscience

[1] Department of Civil Engineering, University of Birmingham, Edgbaston, Birmingham, B15 2TT, UK.

[2] School of Geography, Geology and the Environment, William Smith Building, Keele University, Keele, Staffordshire, ST5 5BG, UK.

[3] Cheshire East Council, Westfields, Middlewich Road, Sandbach, CW11 1HZ

* christopherbrown.private@gmail.com

Keywords: Deep geothermal system, Coaxial borehole heat exchanger, Low-enthalpy system, Finite-difference, Cheshire Basin

Authorship statement: CSB designed the model, analysed data, performed the computations and drafted the manuscript. NC conceived the concept and design of the study, supervised the findings of this work, aiding with technical support and manuscript drafting. SE supervised the findings of this work, aiding with technical support and manuscript drafting. DG supervised the project, aiding with technical support. All authors approved the final manuscript.

Abstract

Few deep wells have been drilled in the Cheshire Basin, resulting in high geological and financial risk of geothermal developments. Although the geothermal gradient in the basin can be predicted, the transmissivity of aquifers at depth are unknown. This has led to an investigation of lower risk strategies such as deep coaxial borehole heat exchangers (BHEs) for spatial heating, rather than traditional doublet methods. A model of a deep coaxial BHE was designed within MATLAB using the finite-difference method. The model produces accurate results in comparison to an analytical solution with a fast computational time. Results indicate that under best case geological parameters sustainable heat loads in excess of 298.7 kW can be produced from deep coaxial borehole heat exchangers at a depth of 2.8 km over the duration of a 20 year operational cycle. The thermal gradient and conductivity for this scenario were set at 27 °C/km and 3 W/m°C, respectively.

The thermal gradient, depth of borehole, volumetric flow rate and thermal conductivity of the surrounding rock all impact the heat load and outlet temperature of a deep coaxial borehole heat exchanger. The coefficient of system performance decreases with increased volumetric flow rates due to an increase in power consumption within the borehole heat exchanger. For an optimal flow rate of 4 l/s (calculated as the flow rate to produce most net power at the end of a heating season), the coefficient of system performance was 5.29. The thermal performance and efficiency of the system provides confidence that the geothermal resource of the Cheshire Basin has significant potential to be developed via deep coaxial borehole heat exchangers. Additionally, regression analysis was undertaken in this study. These models can be used to predict heat loads and outlet temperatures at the end of a heating season without the need for complex numerical modelling.

1. Introduction

Geothermal energy is a renewable energy source capable of replacing some of the energy currently produced from non-renewable sources, such as oil and gas. Geothermal schemes exploiting energy from deep low-enthalpy systems (> 1 km), where heat is transferred from the Earth's hot core towards the cooler surface of the crust and from decay of radionuclides, can often produce more energy than shallow systems (<10 m), where heat is transferred to the Earth by the sun. Shallow systems of 15-500 m in depth typically show an increase in heat corresponding to the natural geothermal gradient (Krarti et al., 1995; Pérez, 2019; Riva, 2019). Geothermal systems also have the benefit of being weather independent (Schiel et al., 2016) and are able to produce a constant base load of energy.

In the UK, the exploitation of deep low-enthalpy geothermal systems is in its infancy, with only one commercial scheme (supplying ~3000 homes, 10 schools and numerous commercial buildings) operating at Southampton (Barker et al., 2000; Energie-Cités, 2001; Lund et al., 2011). At Southampton, a single extracting well targeting the Sherwood Sandstone Group at a depth of ~1.8 km is used to produce the fluid with a submersible pump (Price and Allen, 1984; Barker et al., 2000), discharging the production fluid into the sea (Energie-Cités, 2001). Unfortunately, this disposal method of brine is not always feasible, with the majority of the low-enthalpy prospects in England located inland; meaning either doublet schemes or an alternative method will be required to exploit the energy. Currently, there is a high level of geological and financial risk associated with deep geothermal schemes resulting in limited investment and developments (Hirst et al., 2015). As such, an alternate low-risk strategy is investigated in this paper which focuses on a novel heat extraction method for deep geothermal resources. Deep coaxial borehole heat exchangers (BHEs) are a proven technology used for the extraction of heat from shallow systems (e.g., Acuña and Palm, 2010; Sliwa and Rosen, 2017; Javadi et al., 2019) with interest in their use for deep resources increasing (e.g., Djikshoorn et al., 2013; Law et al., 2014). In populated areas the space to have an array of shallow

BHEs may not be available and as such the feasibility of single deep BHEs must be tested. It has been suggested that deep coaxial BHEs can be used in almost any geological scenario (Law et al., 2014), with cold fluid injected into the annulus, heated by the surrounding subsurface and then the hot fluid is extracted by a circulation pump to the surface in an insulated central pipe, before passing through a heat pump (Fig. 1).

Although BHEs are commonly used in shallow applications (e.g., Nabi and Al-Khoury, 2012a, 2012b), few have explored the potential for use in deep systems. Some studies have attempted to model heat flow for deep coaxial BHEs for UK based case studies (Law et al., 2014; Westaway, 2018), however, the former fails to predict accurate thermal drawdown in the borehole, whilst the latter relies on simplifications to form an analytical solution. Further research has addressed the influence of different parameters on the performance of deep coaxial BHEs globally using numerical and analytical solutions, with studies focused on short performance periods (i.e., 4 months). Both engineering and geological parameters affect the performance of deep coaxial BHEs. The outflow temperature is influenced by: engineering parameters such as flow rate, injection temperature, borehole depth, pipe diameter and thermal conductivity of the inner and outer pipe/grout (Djikshoorn et al., 2013; Fang et al., 1017; Song et al., 2018; Chen et al., 2019; Hu et al., 2019; Liu et al., 2019), and geological parameters such as the thermal gradient and thermal conductivity of the surrounding rocks (Chen et al., 2019). In this study, the finite-difference method was used to model a deep geothermal system in 3D, with the coaxial BHE modelled as a 1D line component to the model surrounded by a 3D geological subsurface (Fig. 1) (Al-Khoury et al., 2005; Al-Khoury and Bonnier, 2006; Al-Khoury, 2011). Using a 1D line source to represent the BHE requires fewer nodes and less computational time. The model was verified against an analytical solution before being used to model heat flow in the Cheshire Basin for short term 4 month seasonal heating simulations and long term simulations of the lifetime of a typical BHE.

By solving the governing equations using the finite-difference method the model in this study offers a reproducible and highly accurate method that can be solved with a fast computational time due to the 1D wellbore component. In comparison, other numerical models have been developed which rely on 2D finite-difference grids (E.g., Djikshoorn et al., 2013) or have a higher level of error (Liu et al., 2019). This study also adds the benefit of producing regression models which can be used to predict seasonal quasi-steady state outlet temperatures and thermal power at the end of a 4 month period without the need for complex numerical models. Although some regression development has been undertaken before for BHEs in Canada (Hu et al., 2019), this study incorporates further parameters specific to the UK and Europe previously not modelled.

The Cheshire Basin was selected as a case study as it contains a significant deep geothermal resource (75 x 10^{18} J – 23 % of the UK's estimated low-enthalpy resources) (Rollin et al., 1995) and has multiple deep wells which it is hypothesised could be converted at low-cost to deep geothermal BHEs (Brown et al., 2019a,b). The Cheshire Basin is located in the northwest of England (Fig. 2), covering an aerial extent of 3500 km^2 (Hirst et al., 2015) and consists of a thick clastic succession of Permo-Triassic sandstones, capped by Triassic mudstones (e.g., Plant et al., 1999). To test the potential for the development of deep coaxial BHEs in the Cheshire Basin volumetric flow rates, borehole depth, thermal gradient and conductivity of the surrounding rocks were modelled for a series of short simulations to investigate the impact of the varying parameters on the achievable heat load. These parameters have been tested for local conditions specific to the Cheshire Basin; many of which are applicable across the UK and Europe. The best and worst performing parameters were then simulated for long term simulations (20 years) to investigate the likely maximum and minimum heat loads achievable and the impact of annual operational cyclicity.

2. Methods

2.1 Governing equations of heat flow in the subsurface

Heat transfer in the subsurface surrounding the BHE is dominated by conductive heat flux. Chen et al. (2019) suggests the influence of groundwater and advection on the performance of deep BHEs to be minimal. As such, heat flux in the rock was modelled as (e.g., Nield and Bejan, 1992; Howell et al.,2021):

$$\frac{\partial T}{\partial t} = \alpha \nabla^2 \mathrm{T} \qquad 1$$

where T is the temperature, t is time and α is the thermal diffusivity of the rock. The symbols and respective property used in the governing equations are listed in table 1.

2.2 Governing equations of heat flow in the coaxial borehole heat exchanger

The boreholes were modelled to account for thermal interactions between the wellbore and the surrounding rock. The model used was first proposed by Al-Khoury et al. (2005) and Al-Khoury and Bonnier (2006) and consists of a series of 1D nodes designed to simulate heat flow in a borehole, incorporating the outer solid rock, grout, pipe and the geothermal fluid in a closed loop system. This model has been widely used and verified for shallow systems (e.g., Al-Khoury et al., 2010; Diersch et al., 2011a, 2011b; Nabi and Al-Khoury, 2012b; Haslam, 2013) and is often referred to as the Dual-Continuum approach (e.g., Hein et al., 2016; Chen et al., 2019). This method reduces computational time, whilst maintaining the physical properties of the wellbore. The 1D approach does, however, fail to model variations in temperature along the horizontal axis for each specific component of the BHE (grout, pipe in, pipe out) (Saeid et al., 2013). This is a sensible assumption as the slimness of these components will result in minor horizontal heat flux. The model incorporates heat flux in the vertical direction across the cross sectional area (left hand side of equations 2-5), whilst thermal resistances are modelled across the horizontal – allowing a significant reduction in spatial discretisation and computational time (Fig. 3a). The heat flux in the horizontal direction shown in figure 3a as Q, is equal to the right hand side of equations 2-5 and acts as a heat source.

When investigating the thermal interactions in a BHE with a central co-axial pipe the heat exchange between the central pipe and annulus can be modelled as (Figs. 1 & 3):

$$\rho_f C_f \frac{\partial T_{po}}{\partial t} A_{po} - \lambda_f \frac{\partial^2 T_{po}}{\partial z^2} A_{po} - \rho_f C_f u_{po} \frac{\partial T_{po}}{\partial z} A_{po} = b_{poi}\left(T_{pi} - T_{po}\right) 2\pi r_{po} \qquad 2$$

$$\rho_f C_f \frac{\partial T_{pi}}{\partial t} A_{pi} - \lambda_f \frac{\partial^2 T_{pi}}{\partial z^2} A_{pi} + \rho_f C_f u_{pi} \frac{\partial T_{pi}}{\partial z} A_{pi} = b_{poi}\left(T_{po} - T_{pi}\right) 2\pi r_{po} + b_{pig}\left(T_g - T_{pi}\right) 2\pi r_{pi} \qquad 3$$

$$\rho_g C_g \frac{\partial T_g}{\partial t} A_g - \lambda_g \frac{\partial^2 T_g}{\partial z^2} A_g = b_{pig}\left(T_{pi} - T_g\right) 2\pi r_{pi} + b_{sg}\left(T_s - T_g\right) 2\pi r_g \qquad 4$$

$$\rho_s C_s \frac{\partial T_s}{\partial t} A_s - \lambda_s \frac{\partial^2 T_s}{\partial z^2} A_s = b_{sg}\left(T_g - T_s\right) 2\pi r_g \qquad 5$$

where the subscript po is for the outlet pipe (central pipe), pi is the inlet pipe (annulus), g is the grout, s is the solid rock mass. T_p is the temperature of the pipe, λ_f is the thermal conductivity of the fluid, b_{pg} is the reciprocal of thermal resistance between the wellbore pipe and grout (e.g., Al-Khoury et al., 2010; Al-Khoury, 2011), b_{sg} is the reciprocal of the contact resistance between the grout and rock, A_g is the area of the grout etc., (table 1). The heat transfer coefficients (R) for the thermal wellbore model can be described using an analogy to electrical circuits (Fig. 3b) (after Al-Khoury et al., 2005; Al-Khoury and Bonnier, 2006; Al-Khoury, 2011). For instance the reciprocal of the contact resistance can be calculated between the outlet pipe and inlet pipe as:

$$b_{poi} = \frac{1}{R_{poi}} \qquad 6$$

where the thermal resistance is calculated as the sum of advective and conductive counterparts.

$$R_{poi} = R_{poconvection} + R_{pipe\ material} + R_{piconvection} \qquad 7$$

The convective components can be calculated as (e.g., Al-Khoury, 2011; Saeid et al., 2013):

$$R_{poconvection} = \frac{1}{r_o / r_i \bar{h}} \qquad 8$$

whilst the thermal resistance in the pipe material can be calculated as:

$$R_{pipe\ material} = \frac{r_o\ ln(r_o/r_i)}{\lambda_p} \tag{9}$$

where r_i is the internal radius of the pipe, r_o is the outer pipe radius and where $\bar{h} = Nu\ \lambda_f/D$. D is the inner diameter of the producing wellbore pipe. Nu is the Nusselt number which can be calculated using the Dittus Boelter correlation (e.g., Saeid et al., 2013). The thermal resistance between other components are similarly calculated, such that the reciprocal of thermal resistances are:

$$b_{pig} = \frac{1}{R_{pig}}, b_{sg} = \frac{1}{R_{sg}} \tag{10}$$

and there corresponding thermal resistances are:

$$R_{pig} = R_{piconvection} + R_{pipe\ material},\ R_{sg} = R_{grout} \tag{11}$$

2.3 Numerical solution and implementation in MATLAB

MATLAB was used for model development due to its fast computational times and visualisation packages. The wellbore was simulated as a 1D nodal line within the geological media, which was discretised as a 3D nodal domain. Heat flow in the subsurface was described using equation 1, whilst the BHE was described using equations 2-5. The 3D spatial domain was discretised explicitly using central differences, whilst the temporal domain was discretised using the forward Euler method. When using MATLAB, the ‘del2’ function was used for approximation of derivatives and the various plot functions can be used for visualisation (e.g., ‘plot’, ‘surf’, ‘contour’ etc.).

When solving for heat flux between the 1D line component and 3D geological model, heat flux is solved horizontally using thermal resistances and vertically using the finite-difference method (Eq. 2-5). The solid rock component represents the adjacent rock volume directly around the BHE

(Eq. 5). These values are then updated for the 1D BHE nodal locations within the 3D model for the solid rock component and are treated as boundary values. The finite-difference method is then used to solve the governing equation (Eq. 1) in the 3D model.

2.4 Verification

The numerical model is verified by comparing the results of a simulation to an analytical solution for fluid movement within a pipe. The analytical solution is typically used to verify BHEs (e.g., Nabi and Al-Khoury, 2012b) and was developed by van Genuchten and Alves (1982). The analytical solution is more simple than the numerical solution, thus some assumptions and simplifications are made: it is assumed that the central production pipe is a perfect insulator (i.e., no heat is transferred) and the production temperature is the same as the bottom-hole temperature, the surrounding rock is a constant temperature, and the model only considers heat transfer through the pipe to the surrounding rock and not the grout. The parameters used are listed in table 2 and the results were compared after a simulation period of 4 months (Fig. 4).

The numerical and analytical solutions have an extremely close fit, with the error increasing with depth. As shown in figure 4, at the end of the simulation the maximum difference in temperature at a depth of 2.8 km is 0.07 °C, which corresponds to an error of 0.17 %. The error was calculated as the percentage error between the numerical and analytical solution. The analytical solution has a slightly elevated temperature in comparison to the numerical model; however, the difference is negligible suggesting that the model is suitable to simulate the performance of deep BHEs.

2.5 Model set up and boundary conditions

2.5.1 Initial conditions and domain boundaries

A series of short simulations designed to test the model over a typical heating season of 4 months were undertaken to establish best and worst case conditions. The model domain was discretised on a non-uniform Cartesian grid which extends from 90 m by 90 m by 3000 m, with the borehole in the centre penetrating to a depth of 2.8 km. Following this, longer simulations designed to test the modelling approach under both best and worst case geological conditions over the lifetime of a BHE (20 years) were undertaken. The thermal propagation away from the BHE was evaluated during the simulations to ensure no boundary interaction occurred and for the 20 year simulation the mesh was expanded to a lateral distance (x,y) of 390 m. A lateral mesh spacing of 1 m was assigned in proximity to the wellbore, expanding laterally away by a factor of 1.2, whilst a vertical mesh spacing of 20 m was chosen. A Cartesian grid was chosen such that in future work the model can be developed further to incorporate multiple BHEs and groundwater flow etc.

It was assumed that at surface level there is no heat flux or interaction with the air at the surface ($\frac{\partial T}{\partial z} = 0$), whilst at the base and lateral boundaries of the model the temperature was assumed constant ($T_z = T_{(z,t=0)}, T_x = T_{(x,t=0),}\ T_y = T_{(y,t=0)}$). At the top of the BHE the inlet temperature was set at ($T_{f(z=0,t)} = T_{in}$) and the outlet temperature was recorded as ($T_{f(z=0,t)} = T_{out}$). Under initial conditions it was assumed the temperature of the fluid in the BHE is in equilibrium with the grout and surrounding rocks in the subsurface ($T_{pi} = T_{po} = T_g = T_s$).

The thermal gradient was assumed to be homogenous and linear, and the parameters of the system are summarised in table 1. The diameter of the borehole was chosen to match those drilled in the UK (taken at 0.306 m to match the Southampton geothermal borehole) (Downing et al., 1984), whilst the central outlet pipe diameter was chosen as 0.05 m to maximise outlet temperatures (Liu et al., 2019). The injection temperature was assumed fixed at 10 °C to investigate the effect of different parameters on heat load and outlet temperature. This is slightly higher than the minimum operational temperature in deep BHEs of 4 °C (Chen et al., 2019) and the values of the grout material are typical of those used in geothermal systems (e.g., Allan, 1997).

2.5.2 Parameterisation

A variety of parameters were modelled to reflect different engineering and geological conditions within the Cheshire Basin, summarised in table 3. A range of boreholes have been drilled from depths of a few metres to a few kilometres with many of these currently unused and 95 % of the well details being confidential (e.g., Hirst, 2017). To reflect this, depths of 0.8 km to 2.8 km were modelled to investigate the potential for retrofitting drilled deep boreholes to coaxial BHEs. The thermal conductivity of the surrounding rock was modelled from a range of 2 - 3 W/m°C which is typical of the thick succession of sandstones and mudstones (Downing and Gray, 1986). To investigate the maximum achievable thermal load, volumetric flow rates of 2 - 12 l/s were modelled, whilst a range of thermal gradients (17 - 27 °C/km) were considered to reflect different thermal regimes (Downing and Gray, 1986; Burley et al., 1980; Plant et al., 1999; Busby, 2014).

2.6 Evaluation of borehole heat exchanger performance

The thermal performance of the coaxial BHE was determined by considering the heat load or thermal power (P) (e.g., Dijkshoorn et al., 2013; Liu et al., 2019):

$$P = \rho_f c_f Q(T_{out} - T_{in}) \qquad 12$$

It is also important to consider the efficiency of the system during long term operational performance. This can be done by calculating the coefficient of performance (COP) which is the ratio of the thermal energy supplied by the borehole heat exchanger (P) and the electrical energy consumed by the heat pump (W_{hp}) (e.g., Kim et al., 2010).

$$COP = \frac{P}{W_{hp}} \qquad 13$$

The COP can be calculated for a system with floor heating at a temperature of 35 °C by assuming a linear relationship with the outlet temperature (Hein et al., 2016):

$$COP = (T_{out} \times 0.083) + 3.925 \qquad 14$$

However, when exploiting geothermal energy from a deep BHE the power from the circulatory pump (W_{cp}) must be considered as there will be a greater pressure drop in comparison to shallow BHEs, thus more energy is required to circulate the fluid. As such, the coefficient of system performance (CSP) can be used to evaluate the total electrical energy used by the system to extract the heat (Chen et al., 2019):

$$CSP = \frac{P}{W_{hp} + W_{cp}} \tag{15}$$

The energy consumed by the circulating pump can be calculated as (Liu et al., 2019):

$$W_{cp} = \frac{\Delta P \times Q}{n} \tag{16}$$

where ΔP is the pressure drop in the BHE, Q is the volumetric flow rate and n is the efficiency of the pump (assumed to be 75 %). The change in pressure along the coaxial BHE can be calculated as (Gordon et al., 2018):

$$\Delta p = \frac{\rho_f F_i L V_i^2}{4 r_i} + \frac{\rho_f F_o L V_o^2}{4 r_o} \tag{17}$$

where F_i is the Darcy friction factor of the inlet, L is the length of the pipe, V_i is the velocity of the inlet and r_i is the radius of the inlet.

3. Results

When the BHE was simulated with the initial fixed parameters (i.e., table 1), the outlet temperature and heat load rapidly dropped within the first 5 days, with minimal change after 10 days as the thermal power and outlet temperature began to level off in an exponential decline (Fig. 5a). The initial outlet temperature reached a high of 48.8 °C and thermal power of 652.4 kW in the first hour. At the end of the simulation the outlet temperature was 24.04 °C and the heat load was 235.6 kW.

Similarly, the temperature of the fluid along the annulus and central production pipe rapidly decreases as the 10 °C inlet fluid temperature creates thermal drawdown within the BHE (as shown in Fig. 5b). At the start of the simulation the fluid at the base of the BHE was 80 °C, whilst after 30 days declined to 37.11 °C and at the end of the 4 month period was 33.66 °C. The high thermal conductivity outer piping allows rapid heat transfer to warm the fluid in the annulus, whilst the low thermal conductivity of the inner production pipe insulates the warm fluid, limiting heat loss. The heat flux from the grout into the annular pipe is rapid in the first few days, increasing with depth, whilst significantly reducing towards the end of the simulation period (Fig. 5c & d). The grout has a reduced thermal conductivity compared to the outer pipe which limits the heat flux into the borehole; however, this is only minor as the base of the grout has a maximum of 0.55 °C difference to the circulating fluid. Given that the input temperature is equal to the ground surface temperature, energy is always gained in the deep BHE. In reality, seasonal effects (i.e., cooling during winter) may lead to energy being lost in the upper few hundred metres. Radially around the borehole the maximum thermal propagation is 15 m, with the most change (more than 0.01 °C from static conditions) within 10 m of the BHE (Fig. 6). The thermal flux in the subsurface is characterised by sharp concave coning upwards around the BHE, shallowing towards the surface (Fig. 6).

3.1 Influence of borehole depth

Borehole depths were investigated from 0.8 - 2.8 km. The reduction in borehole depth limits the maximum extractable energy as the bottom-hole temperature is reduced (assuming the gradient is linear). Both the thermal power and outlet temperature both increase with depth. Regression analysis highlights that a polynomial fit with a high level of accuracy can be observed (Fig. 7a). As the depth of the BHE approaches zero the outlet temperature is asymptotic to the inlet/surface temperature and the thermal power to zero. This is due to the heat load being determined by the difference between the inlet and outlet temperatures. The minimum heat load is observed in the 0.8 km deep borehole at 20.58 kW and the maximum is observed in the 2.8 km borehole at 235.6 kW.

3.2 Influence of thermal conductivity of the confining strata

Thermal conductivity values of 2 - 3 W/m°C were investigated due to the vast variations in lithological composition between mudstones, sandstones and marls within the basin (Downing and Gray, 1986). As shown in figure 7b, the final outlet temperature and heat load have a logarithmic increase proportional to higher thermal conductivities. This is due to the higher thermal conductivities allowing the surrounding rock to replenish heat stores in the BHE. The heat load at the end of the simulation period increases with thermal conductivity from 235.6 kW to 288.1 kW and outlet temperature from 24.02 °C to 27.15 °C.

3.3 Influence of thermal gradient

A range of thermal gradients were modelled to reflect the range in predicted temperature gradients in the basin (Downing and Gray, 1986; Burley et al., 1980; Plant et al., 1999; Busby, 2014). The higher thermal gradients modelled resulted in increased outlet temperature at the end of the simulation. Figure 8a, shows a positive linear relationship fitted between thermal gradients and the final outlet temperatures. This is due to there being a higher initial bottom-hole temperature and therefore, a greater maximum heat load at the base of the BHE. The produced heat load at the end of the simulation increases between the minimum and maximum thermal gradients from 160.2 kW to 254.4 kW, respectively (Fig. 8a). Similarly, for outlet temperatures an increase is observed of 19.54 °C to 25.15 °C.

3.4 Influence of volumetric flow rates

Flow rates were increased incrementally by 2 l/s, from 2 to 12 l/s. Analysis showed an exponential decline in outlet temperature corresponding to increasing flow rates. This is due to an increase in thermal drawdown in the borehole and cooling of the surrounding rocks. In contrast, the final thermal power had a high-order polynomial fit. In figure 8b, a rapid increase in thermal power was observed before a slight decline. This highlights the reduction in outlet temperature is limiting the heat load. The highest and lowest final outlet temperatures were 15.09 °C and 29.72 °C, whilst the flow rate that produced most energy was identified as 8 l/s (Fig. 8b).

3.5 Impact of parameters on the coefficient of performance

When addressing the overall efficiency of a system both the depth of the BHE and the volumetric flow rate most significantly impact the coefficient of performance (COP) (Fig. 9a). Increased volumetric flow rates reduce the COP due to cooler outlet temperatures observed at the end of production. This results in the heat pump requiring more energy to use the extracted heat. Increased borehole depths show higher COPs for deeper boreholes due to the higher outlet temperatures. Both thermal conductivity and thermal gradient result in an increase of COP that is proportional to higher outlet temperatures caused by the respective properties.

When considering the energy used to pump the fluid through the BHE, the overall coefficient of system performance (CSP) is reduced for all scenarios. Similarly to the COP, the CSP for the thermal gradient and conductivity marginally increases with better respective properties, however, it shows an overall decrease to the COP by >1 (Fig. 9b). Although the depth of the BHE has a significant impact on the efficiency of the BHE, the volumetric flow rate has the greatest effect on the CSP, reducing the efficiency with higher flow rates. The highest flow rate measured in this study resulted in the COP reducing from 5.17 to 2.22. The energy required to pump the fluid in the system for the greatest flow rates equates to 66.3 kW, whilst the energy required for the heat pump was 49.5 kW. This shows that high volumetric flow rates are ineffective due to their high electrical energy consumption. From this the total useable energy was calculated (i.e., $P - (W_{hp} + W_{cp})$) which showed an increase in the useable energy correlated to more efficient BHEs, however, for volumetric flow rate the highest total energy was established for the flow rate of 4 l/s (Fig. 9c).

3.6 Long term analysis of achievable heat loads

Analysis of the combined best and worst performing parameters (i.e., the highest and lowest total useable energy (fig. 9c)) for thermal conductivity of the confining rock and thermal gradient was undertaken to consider the varying achievable heat load. Both controllable engineering parameters (borehole depth and flow rate) were fixed at optimal conditions at 2.8 km and 4 l/s for both scenarios, whilst the inlet temperature remained constant. The simulation period lasted for 20 years and consisted of 4 months of production (considered as the heating season) and 8 months of recovery. In the UK, a typical heating season can last between 4 and 9 months (BRE, 2013). In this study, we chose the former period as a heating season to investigate the impacts of longer recharge time, and for consistency and comparison with the short term simulations. Additionally, it is worth noting in reality the BHE may have a small capacity for use outside the heating season. This is not modelled in this paper as the low-season demand is sporadic in towns overlying the Cheshire Basin (Arup, 2018).

3.6.1 Analysis of the first production cycle

Within the first hour the initial production temperature rapidly increased for the optimal scenario to 50.93 °C producing a power of 687.6 kW, followed by a rapid decline in both power and temperature (Fig. 10). At the end of the four month production period the temperature began to stabilise at 28.58 °C producing 312.1 kW of energy.

In contrast the worst case scenario utilised a reduced thermal gradient of 17 °C/km, resulting in far lower production temperatures and heat loads. The poor thermal conductivity of the confining rock also limits the ability for heat to be transmitted to the BHE. Similarly to the best case scenario, a rapid increase in temperature within the first hour was followed by an exponential drop in production temperature over the four months. At the end of production period the outlet temperature was 19.57 °C, producing 160.6 kW of energy (Fig. 10).

3.6.2 Analysis of annual cyclicity

The maximum outlet temperatures during the production cycles reduce within the first few years of operation (Figs. 11 & 12). The maximum outlet temperature within the first four operational cycles drops by 1.66 °C and 1.47 °C respectively, for the best and worst case scenarios, whilst over the next 16 cycles the temperature drop is only 0.7 °C and 0.54 °C. This highlights during operation and recovery of the BHE, the thermal field in the subsurface is nearing equilibrium, particularly in the last few years of BHE operation when the change in maximum outlet temperature for both cases is minor. Interestingly, over the lifetime of a BHE the lowest outlet temperature during the operational periods only changed by 0.81 °C and 0.57 °C, respectively. This is reflected in the change in minimum heat loads over the 20 year production period. For the best case scenario the heat load at the end of operational cycles reduces between year 1 and 20 from 312.1 kW to 298.7 kW, whilst the worst case scenario heat load at the end of operational cycles reduces from 160.6 to 151.3 kW. This suggests that over the 20 year production period heat loads of between 298.7 kW and 151.3 kW can be sustainably extracted depending on the geology. The radial propagation of heat away from the BHE also varies between cases. The low-thermal conductivity limits the transmission in heat away from the BHE and recharge with a maximum radial thermal drawdown of 75 m in the worst case scenario, whilst in the best case scenario, the maximum cooling is seen to 90 m away from the BHE (to within 0.01 °C of static conditions).

3.6.3 Analysis of the coefficient of performance (COP) and coefficient of system performance (CSP)

Under the optimal scenario for the performance of BHEs, the COP is in excess of 6.29 for the duration of the 20 year simulation. For the worst case scenario the COP is in excess of 5.55. When considering the additional power of the circulatory pump the CSP decreases for both scenarios to 5.29 and 4.17, respectively. This corresponds to an electrical consumption of 56.4 kW and 36.2 kW, highlighting for deeper systems the circulating pump consumes a significant amount of energy and the additional pumping power can have the most significant impact on the CSP.

4. Discussion

4.1 Modelling methodology and regression analysis

This study has highlighted that the finite-difference model developed can be simulated in a reasonably fast computational time (typically under 10 minutes for a 4 month heating period) to a high degree of accuracy (error within 0.17 %). In comparison to other numerical models developed for deep coaxial BHEs, the accuracy is significantly improved. The maximum relative error is 0.17 %, whilst in other similar numerical models the errors observed reach a maximum of 11.3 %, 2.4 % and 1.74 % (Liu et al., 2019; Chen et al., 2019; Hu et al., 2019, respectively). For the latter, it could be due to the increased simulation periods with the model tested for a duration of 25 years. In comparison to analytical solutions, the modelling method also considers all system components such as grout and piping which are often neglected in analytical solutions (e.g., Westaway, 2018).

Although the modelling methodology has some clear benefits, such as computational speed and accuracy, there are some further considerations required for future long term modelling. The boundary conditions used in this study for the lateral boundaries and base of the model were fixed at a constant temperature, whilst at the surface level there was no heat flux or interaction with air. During the simulations, the interactions were carefully monitored to ensure no inaccuracies were caused by the boundaries, and testing of lateral and basal distances from the borehole was undertaken. Further long term modelling may benefit from the incorporation of a constant heat flux through the basal boundary to replicate the Earth's natural geothermal gradient. Additionally, interactions between the upper surface of the model and atmosphere may help to incorporate the true effects of seasonal variations.

The regression analysis conducted (figures 7 and 8) can provide reliable estimators for outlet temperature and heat loads. The analysis allows values for parameters outside the range tested in this paper to be modelled quickly via a single calculation, with high reliability. The regression models have high R^2 values in excess of 0.9964 which indicate the fitted curves account for 99 % of the data, whilst for thermal gradients the linear fit will always equal the observed values (R^2 = 1). The maximum residual values for both temperature and heat load were observed in the regression models for volumetric flow rate and borehole depth, respectively, with residuals reaching 0.461 °C and 2.29 kW. Although the variance and residual is low in all models the limitation resides when predicting heat load for varying flow rate. The polynomial fit is of a high order (4th) which suggests that further unknown data may not fit accurately.

4.2 Operational influence on a borehole heat exchanger

Borehole depth and volumetric flow rate are engineering parameters that can be pre-determined to improve the efficiency and performance of coaxial BHEs. By increasing the borehole depth a higher thermal load, due to hotter temperatures in the subsurface, can be achieved. Similarly, this is reflected with deeper boreholes corresponding to greater coefficients of performance.

In contrast to borehole depth, where a positive trend is observed between the performance and depth, more consideration is required to identify optimal volumetric flow rates. COP and CSP decreases with increasing volumetric flow rate, showing poorer operational performance. When investigating the net power (i.e., figure 9c), the peak heat load is 4 l/s. This is due to a higher thermal power being achieved in relation to the power required for circulation and operation of the heat exchanger. Careful consideration of operational requirements must be undertaken to achieve high performance of deep coaxial BHEs. Operational parameters can also be used to compensate for poor geological conditions.

4.3 Geological influence on a borehole heat exchanger

The thermal conductivity and thermal gradient in the subsurface are extremely important to the efficiency of a system, as demonstrated in both short and long term simulations. Under the best and worst case scenarios for the lifetime evaluations of a BHE the heat load and CSP significantly reduced by 50.6 % and 21.2 %, respectively. This highlights planning and testing of the subsurface is still required to evaluate the potential for development of deep coaxial BHEs. Although engineering parameters are significant during development these can be pre-determined values, whilst the geological variables can be unknown. Additionally, higher thermal gradients and thermal conductivities may allow for the reduction of drill depth of a BHE, leading to lower investment costs.

4.4 Implications of borehole heat exchanger performance in the Cheshire Basin

The results of this study show heat loads for an operational period of 20 years can be obtained in excess of 298.7 kW, indicating the Cheshire Basin to have a significant potential for geothermal exploitation using the deep coaxial BHE method. As previously discussed, the thermal conductivity and gradients must be considered, particularly when developing in the Cheshire Basin. Lower thermal conductivity materials and gradients are constrained to the near surface level due to the clay rich Mercia Mudstone Group capping the top of the basin (<1.6 km at Prees-1 and Knutsford boreholes) (Mikkelsen and Floodpage, 1997). This means shallower boreholes will have poorer geological characteristics limiting the thermal recharge of a BHE. In contrast, deeper boreholes will penetrate a thick succession of sandstones resulting in greater recharge ability and higher outlet temperatures and thermal loads. Therefore, not only the geological properties must be considered but also the positioning of geological intervals.

The COP of the heat pump for both best and worst case lifetime evaluations is fairly well performing and similar to other deep and shallow BHE studies which typically range from 2 – 6 (e.g., Sanner et al., 2003; Luo et al., 2015; Hein et al., 2016; Li et al., 2017; Gordon et al., 2018; Chen et al., 2019; Nian et al., 2019), however, some suggest that the COP in deep coaxial BHEs can reach closer to 50 with optimisation (Liu et al., 2019). In contrast, when considering the inclusion of the circulatory pump the CSP decreases by up to 57 % of the original COP under high flow rates. This indicates the circulatory pump utilises far more energy for deep BHEs with higher flow rates than shallow BHEs. Therefore, the electrical consumption must also be considered rather than thermal power alone.

Furthermore, the results of the modelling study indicate that under a suitable economic and geological scenario deep coaxial BHEs can be used to develop mid-deep geothermal resources in the Cheshire Basin. The lack of data from deep boreholes limits the potential for investment of using conventional extraction methods (i.e., open-loop doublets); however, the novel alternate method presented here is a possible option for meeting the demand of small towns overlying the basin. In the Cheshire Basin hundreds of water abstraction and hydrocarbon exploration wells have been drilled from the surface level to depths of a few kilometres (with only two exceeding the depths in this study (UKOGL, 2019)). Although many of the hydrocarbon exploration wells are plugged and abandoned, there remains a potential to retrofit these as coaxial BHEs if a cost effective method is found for repurposing. The model can also be used across the UK to evaluate the use of deep coaxial BHEs to meet local demand. The consideration of deep BHE arrays and optimal spacing must be considered for larger developments, however, the small zone of influence around the BHEs suggest they can be spaced within a few hundred metres of each other without interference.

5. Conclusion

In this paper a numerical model was developed for coaxial BHEs using the 1D line source method of Al-Khoury et al. (2005), Al-Khoury and Bonnier (2006) Al-Khoury, (2011) using the finite-difference method. The modelling approach used in this paper was verified to ascertain an extremely high level of accuracy with a maximum error of 0.17 %. Subsequently, the model was used to investigate the potential use of deep coaxial BHEs to develop geothermal energy in the Cheshire Basin, UK. Analysis of a range of engineering and geological parameters were modelled, followed by a best and worst case geological scenario. The key conclusions were:

- Heat flux in the BHE is dominated by vertical changes in fluid temperature within both the central outlet pipe and annular space. An initial rapid increase in outlet temperature is followed by an exponential decline. The radial heat flux is minimal and mostly constrained to the near few metres, with the surrounding rock >10 m undisturbed from static conditions.

- Regression analysis shows the key geological and engineering parameters can be fitted to a polynomial, logarithmic, exponential or linear equation to predict the outlet temperature and heat load at the end of a simulation period. Borehole depth and flow rate can be fitted against a polynomial curve; thermal conductivity of the surrounding rock matched a logarithmic fit and thermal gradient a linear fit. The regression models also have the benefit that they can be used for this specific case study without complex numerical models.
- Higher volumetric flow rates lead to lower outlet temperatures, whilst the optimal volumetric flow rate in this study giving the most energy after consideration of electrical consumption for the heat pump and circulation pump was 4 l/s.
- High volumetric flow rates and increased depth of BHEs can lead to poor efficiency of a system and a reduced coefficient of system performance, and, as such, must be considered during the optimisation of a deep BHE.
- Under best case geological parameters heat loads of 298.7 kW were achieved, whilst under the worst case scenarios heat loads were 151.3 kW.
- If a cost efficient method for converting plugged or unused wells to coaxial BHEs can be achieved in the area then the Cheshire Basin has a significant opportunity to utilise deep geothermal energy.

Funding

We would like to show appreciation to the Natural Environment Research Council (NERC grant reference number NE/M00998X/1) and Cheshire East Council for funding this research.

Computer Code Availability

The finite-difference code was developed by C. S. Brown (email: christopherbrown.private@gmail.com, address: School of Civil Engineering, University of Birmingham, Edgbaston, Birmingham, B15 2TT, UK, telephone: +44(0)121 414 3344) on MATLAB and has been made available from the GitHub repository https://github.com/CSBROWN125/CBASIN-PAPER. The hardware required, software required, program language, program size and how to access the code are available on the website.

References

Acuña, J. and Palm, B., 2010, April. A novel coaxial borehole heat exchanger: description and first distributed thermal response test measurements. In Proceedings of the World Geothermal Congress (p. 7).

Al-Khoury R., 2011. Computational modeling of shallow geothermal systems. CRC press.

Al-Khoury, R., Bonnier, P.G., Brinkgreve, B.J., 2005. Efficient finite element formulation for geothermal heating systems. Part I: steady state. *International Journal for Numerical Methods in Engineering* 63, 988–1013. doi:10.1002/nme.1313

Al-Khoury, R., Bonnier, P.G., 2006. Efficient finite element formulation for geothermal heating systems. Part II: transient. *International Journal for Numerical Methods in Engineering* 67, 725–745. doi:10.1002/nme.1662

Al-Khoury, R., Kolbel, T., Schramedei, R., 2010. Efficient numerical modeling of borehole heat exchangers. *Computer and Geosciences* 36 (10), 1301–1315. doi:10.1016/j.cageo.2009.12.010

Allan, M.L., 1997. Thermal conductivity of cementitious grouts for geothermal heat pumps. BNL, 65, 129. doi:10.2172/573177

Arup, 2018. Technical feasibility report – Crewe Town Centre Heat Network.

Barker, J.A., Downing, R.A., Gray, D.A., Findlay, J., Kellaway, G.A., Parker, R.H., Rollin, K.E., 2000. Hydrogeothermal studies in the United Kingdom. *Quarterly Journal of Engineering Geology and Hydrogeology*, 33(1), 41-58. doi.:10.1144/qjegh.33.1.41

BRE 2013, Report 4: Main heating systems – Follow-Up Survey 2011. A report prepared by BRE on behalf of the Department of Energy and Climate Change. December 2013. BRE report number 286733a.

Brown, C.S., Cassidy, N., Egan, S., Griffiths, D., 2019b. Evaluating the Response of Geothermal Reservoirs in the Cheshire Basin: A Parameter Sensitivity Analysis. In: 2019 AAPG Annual Convention and Exhibition, May 19-22, San Antonio, Texas.

Brown, C.S, Cassidy, N., Egan, S., Griffiths, D., 2019a. Modelling low-enthalpy deep geothermal reservoirs in the Cheshire Basin, UK as a future renewable energy source. In Geophysical Research Abstracts (Vol. 21).

Burley, A.J., Smith, I.F., Lee, M.K., Burgess, W.G., Edmunds, W.M., Arthur, M.J., Bennett, J.R.P., Carruthers, R.M., Downing, R.A., Houghton, M.T., 1980. Preliminary Assessment of the Geothermal Potential of the United Kingdom, in: Strub, A.S., Ungemach, P. (Eds.), Advances in European Geothermal Research. Springer Netherlands, 99–108.

Busby, J., 2014. Geothermal energy in sedimentary basins in the UK. Hydrogeology journal, 22(1),129-141. doi:10.1007/s10040-013-1054-4

Chen, C., Shao, H., Naumov, D., Kong, Y., Tu, K. and Kolditz, O., 2019. Numerical investigation on the performance, sustainability, and efficiency of the deep borehole heat exchanger system for building heating. *Geothermal Energy*, *7*(1), p.18. doi:10.1186/s40517-019-0133-8

Dijkshoorn, L., Speer, S. and Pechnig, R., 2013. Measurements and design calculations for a deep coaxial borehole heat exchanger in Aachen, Germany. *International Journal of Geophysics*, *2013*. doi:10.1155/2013/916541

Downing, R. A., Allen, D. J., Barker, J. A., Burgess, W. G., Gray, D. A., Price, M., Smith, I. F., 1984. Geothermal exploration at Southampton in the UK: a case study of a low enthalpy resource. *Energy exploration & exploitation*, 2(4), 327-342.

Downing, R.A., Gray, D.A., 1986. Geothermal Energy The potential in the United Kingdom. BGS, National Environment Research Council.

Energie-Cités, 2001. Geothermal Energy District heating scheme Southampton (United Kingdom). Case study prepared with the City of Southampton. https://geothermalcommunities.eu/assets/elearning/5.13.SOUTH_EN.PDF

Fang, L., Diao, N., Shao, Z., Zhu, K., Fang, Z., 2018. A computationally efficient numerical model for heat transfer simulation of deep borehole heat exchangers. Energy and Buildings, 167, pp.79-88. doi:10.1016/j.enbuild.2018.02.013

Gordon, D., Bolisetti, T., Ting, D.S. and Reitsma, S., 2018. Experimental and analytical investigation on pipe sizes for a coaxial borehole heat exchanger. *Renewable energy*, *115*, pp.946-953. doi:10.1016/j.renene.2017.08.088

Haslam, S. R., 2013. Informing the practice of ground heat exchanger design through numerical simulations (Master's thesis, University of Waterloo).

Hein, P., Kolditz, O., Görke, U.-J., Bucher, A., & Shao, H., 2016. A numerical study on the sustainability and efficiency of borehole heat exchanger coupled ground source heat pump systems. Applied Thermal Engineering, 100, 421–433. doi:10.1016/j.applthermaleng.2016.02.039

Hirst, C.M., Gluyas, J.G., Adams, C.A., Mathias, S.A., Bains, S., Styles, P., 2015. UK Low Enthalpy Geothermal Resources: the Cheshire Basin. Proc. World Geotherm. Congr. 2015.

Hirst, C.M., 2017. The Geothermal Potential of Low Enthalpy Deep Sedimentary Basins in the UK, PhD thesis, Durham University.

Howell, L., Brown, C.S. and Egan, S.S., 2021. Deep geothermal energy in northern England: Insights from 3D finite difference temperature modelling. Computers & Geosciences, 147, p.104661.

Hu, X., Banks, J., Wu, L., Liu, W.V., 2019. Numerical modeling of a coaxial borehole heat exchanger to exploit geothermal energy from abandoned petroleum wells in Hinton, Alberta. Renewable Energy. doi:10.1016/j.renene.2019.09.141

Javadi, H., Ajarostaghi, S.S.M., Rosen, M.A. and Pourfallah, M., 2019. Performance of ground heat exchangers: A comprehensive review of recent advances. *Energy*, *178*, pp.207-233.

Kim, S.K., Bae, G.O., Lee, K.K., Song, Y., 2010. Field-scale evaluation of the design of borehole heat exchangers for the use of shallow geothermal energy. *Energy*, *35*(2), pp.491-500. doi:10.1016/j.energy.2009.10.003

Krarti, M., Lopez-Alonzo C., Claridge D.E., Kreider J.F. 1995. Analytical Model to Predict Annual Soil Surface Temperature Variation. Journal of Solar Energy Engineering 117(2). 91-99.

Law, R., Bridgland, D., Nicholson, D., Chendorain, M., 2014. Heat extraction from deep single wells. In *Proceedings Thirty-Ninth Workshop on Geothermal Reservoir Engineering Stanford University, Stanford, California.*

Li, C., Mao, J., Zhang, H., Li, Y., Xing, Z., Zhu, G., 2017. Effects of load optimization and geometric arrangement on the thermal performance of borehole heat exchanger fields. *Sustainable cities and society*, *35*, pp.25-35.

Liu, J., Wang, F., Cai, W., Wang, Z., Wei, Q., Deng, J., 2019. Numerical study on the effects of design parameters on the heat transfer performance of coaxial deep borehole heat exchanger. Int J Energy Res.;1–16. doi:10.1002/er.435716LIUETAL.

Lund, J.W., Freeston, D.H., Boyd, T.L., 2011. Direct utilization of geothermal energy 2010 worldwide review. Geothermics, 40(3),159-180. doi:10.1016/j.geothermics.2011.07.004

Luo, J., Rohn, J., Bayer, M., Priess, A., Wilkmann, L., Xiang, W., 2015. Heating and cooling performance analysis of a ground source heat pump system in Southern Germany. *Geothermics*, *53*, pp.57-66. doi:10.1016/j.geothermics.2014.04.004

Mikkelsen, P.W., Floodpage, J.B., 1997. The hydrocarbon potential of the Cheshire Basin. Geol. Soc. Lond. Spec. Publ. 124, 161–183. doi:10.1144/GSL.SP.1997.124.01.10

Nabi, M., Al-Khoury, R., 2012a. An efficient finite volume model for shallow geothermal systems. Part I: Model formulation. *Computers & Geosciences*, 49, 290-296. doi:10.1016/j.cageo.2012.03.019 261

Nabi, M., Al-Khoury, R., 2012b. An efficient finite volume model for shallow geothermal systems—Part II: Verification, validation and grid convergence. *Computers & Geosciences*, 49, 297-307. doi: 10.1016/j.cageo.2012.03.023

Nian, Y.L., Cheng, W.L., Yang, X.Y., Xie, K., 2019. Simulation of a novel deep ground source heat pump system using abandoned oil wells with coaxial BHE. *International Journal of Heat and Mass Transfer*, *137*, pp.400-412. doi:10.1016/j.ijheatmasstransfer.2019.03.136

Nield, D. A., Bejan A., 1992. Convection in a Porous Media, 408, Springer-Verlag, New York.

Pérez, R.E., 2019. Shallow geothermal energy: Geological energy for the ecological transition and its inclusion in European and national energy policies. *European Geologist European Geologist*, p.28.

Plant, J.A., Jones, D.G., Haslam, H.W. eds., 1999. The Cheshire Basin: basin evolution, fluid movement and mineral resources in a Permo-Triassic rift setting. British Geological Survey.

Price, M., Allen, D. J., 1984. The use of pumping tests to evaluate a geothermal reservoir-the Triassic sandstones at Marchwood, Southampton. Proceedings of the Institution of Civil Engineers, 76(3), 697-711.

Rivas, P. 2019. Calefacción por Geotermia. La Energía Renovable del Suelo.

Rollin, K.E., Kirby, G.A., Rowley, W.J., Buckley, D.K., 1995. Atlas of Geothermal Resources in Europe: UK Revision. Technical Report WK/95/07, British Geological Survey, Keyworth.

Sanner, B., Karytsas, C., Mendrinos, D., Rybach, L., 2003. Current status of ground source heat pumps and underground thermal energy storage in Europe. *Geothermics*, *32*(4-6), pp.579-588. doi:10.1016/S0375-6505(03)00060-9

Schiel, K., Baume, O., Caruso, G. and Leopold, U., 2016. GIS-based modelling of shallow geothermal energy potential for CO2 emission mitigation in urban areas. *Renewable Energy*, *86*, pp.1023-1036.

Sliwa, T. and Rosen, M.A., 2017. Efficiency analysis of borehole heat exchangers as grout varies via thermal response test simulations. *Geothermics*, *69*, pp.132-138.

Song, X., Wang, G., Shi, Y., Li, R., Xu, Z., Zheng, R., Wang, Y., Li, J., 2018. Numerical analysis of heat extraction performance of a deep coaxial borehole heat exchanger geothermal system. *Energy*, *164*, pp.1298-1310. doi:10.1016/j.energy.2018.08.056

Van Genuchten, M. T., Alves, W. J., 1982. Analytical solutions of the one-dimensional convective dispersive solute transport equation (No. 157268). United States Department of Agriculture, Economic Research Service.

Westaway, R., 2018. Deep Geothermal Single Well heat production: critical appraisal under UK conditions. Quarterly Journal of Engineering Geology and Hydrogeology, 51(4), 424-449. doi:10.1144/qjegh2017-029

UKOGL, 2019. Website last accessed on January 2019. https://ukogl.org.uk/map/?e=-282393,7032566,-262519,7043630&l=1431655429,81,0&f=14,136,-267870,7038088&b=3&sm=true

Figures

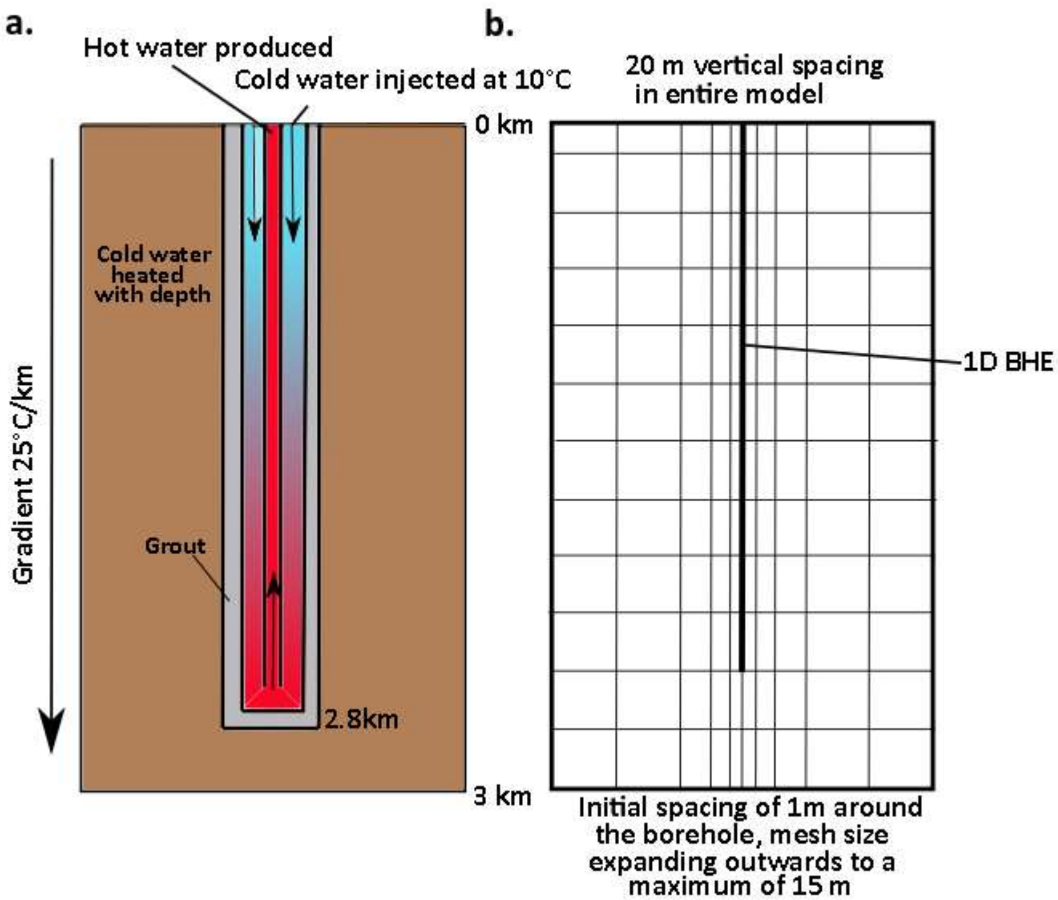

Figure 1. (a) 2D schematic of a closed loop coaxial borehole heat exchanger and (b) schematic of a 2D cross section through the 3D model of the discretisation of the finite-difference grid.

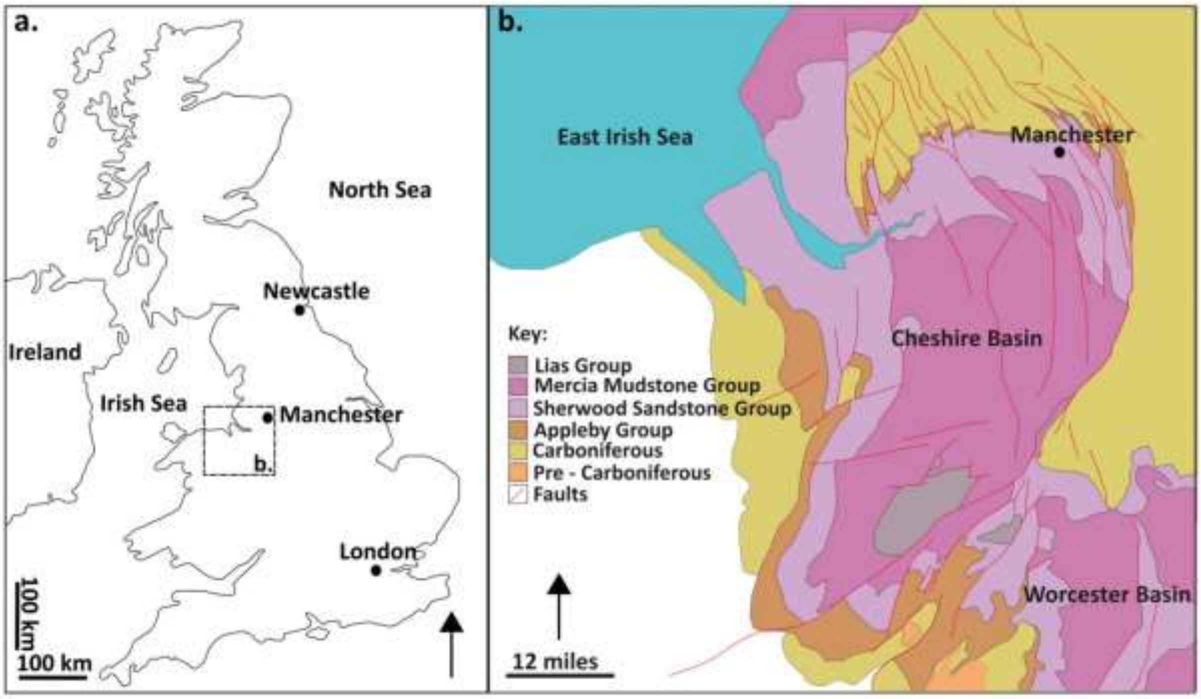

Figure 2. (a) Study area location in the UK and (b) geological outcrop map of the Cheshire Basin (after Plant et al., 1999; Hirst et al., 2015; UKOGL, 2019).

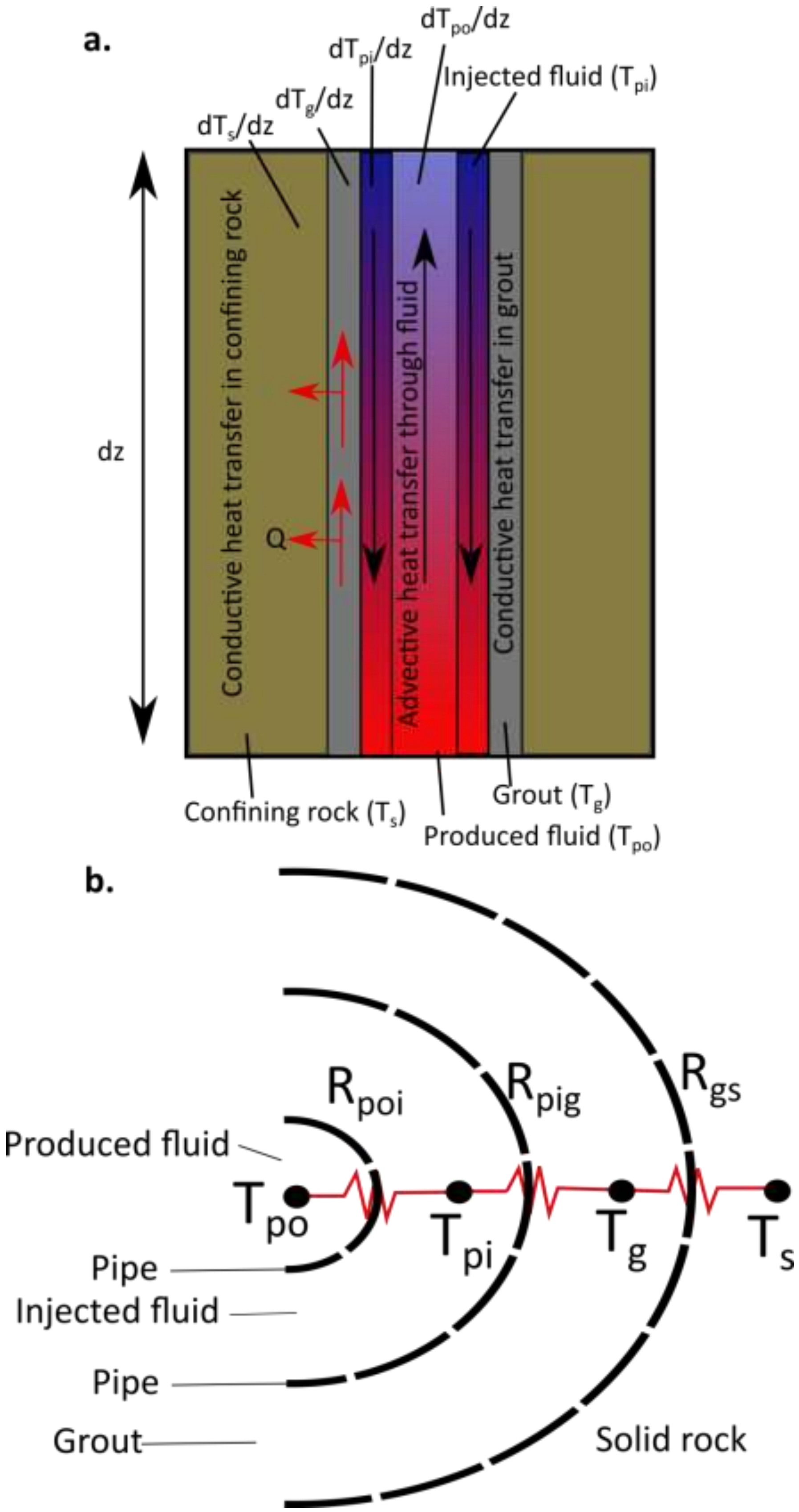

Figure 3. (a) Heat fluxes through the different components of the 1D borehole model. (b) Thermal resistance model through a cross section of the deep coaxial borehole heat exchanger.

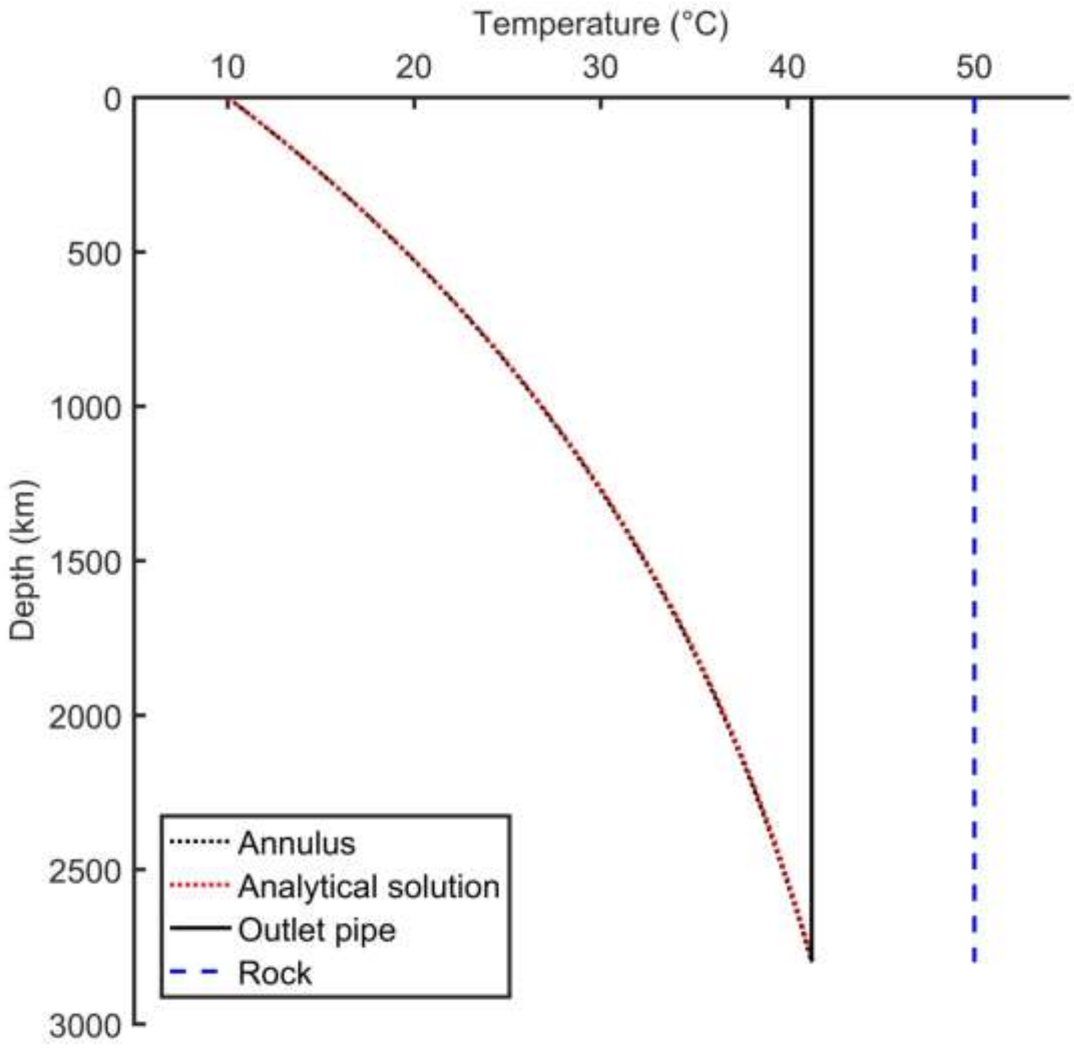

Figure 4. Analytical verification of the numerical solution for deep borehole heat exchangers. Parameters summarised in table 2.

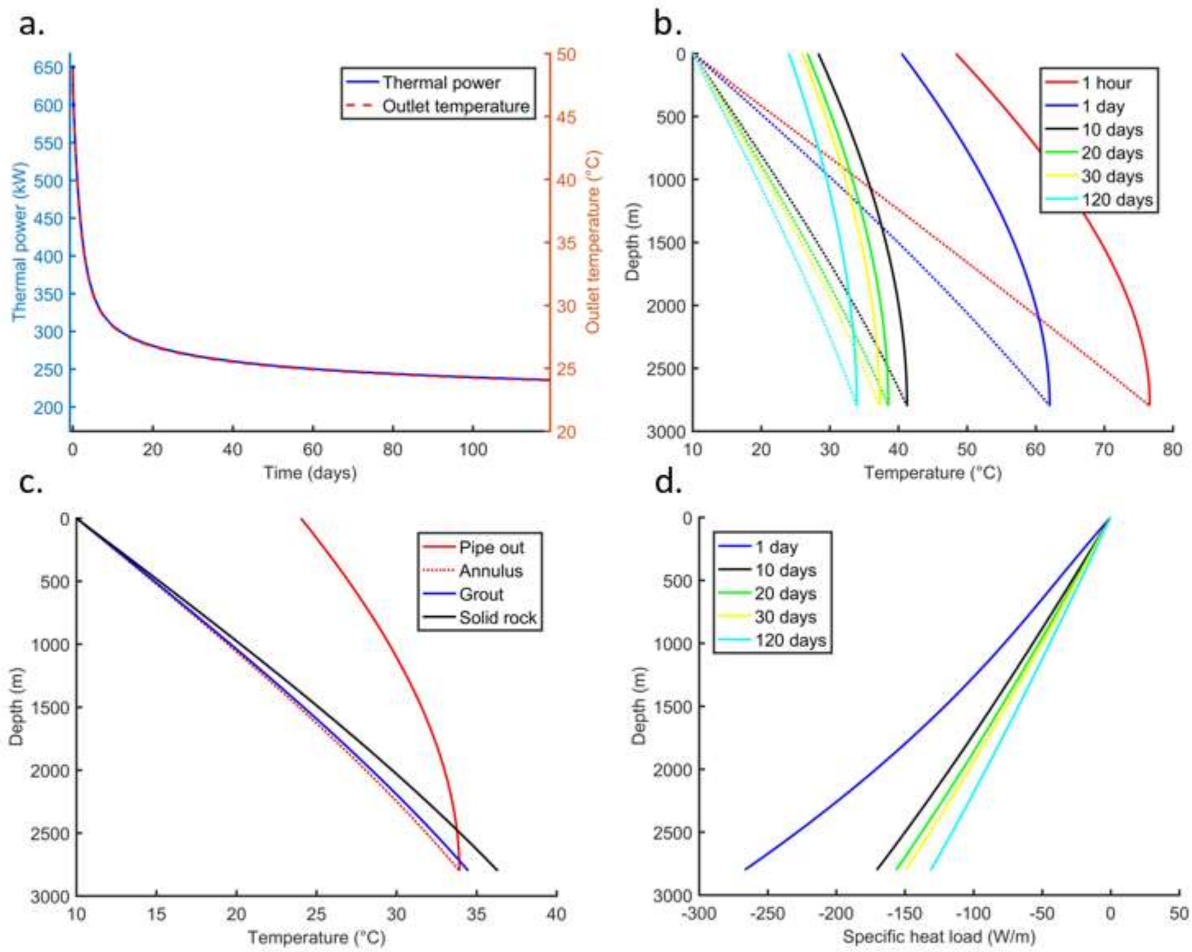

Figure 5. (a) Thermal power and outlet temperature change with time, (b) temperature changes in the annulus (solid line) and central pipe (dashed line) for various times, (c) temperature in the pipe out, annulus, grout and surrounding rock and (d) the specific heat load into the outer annular space at various times.

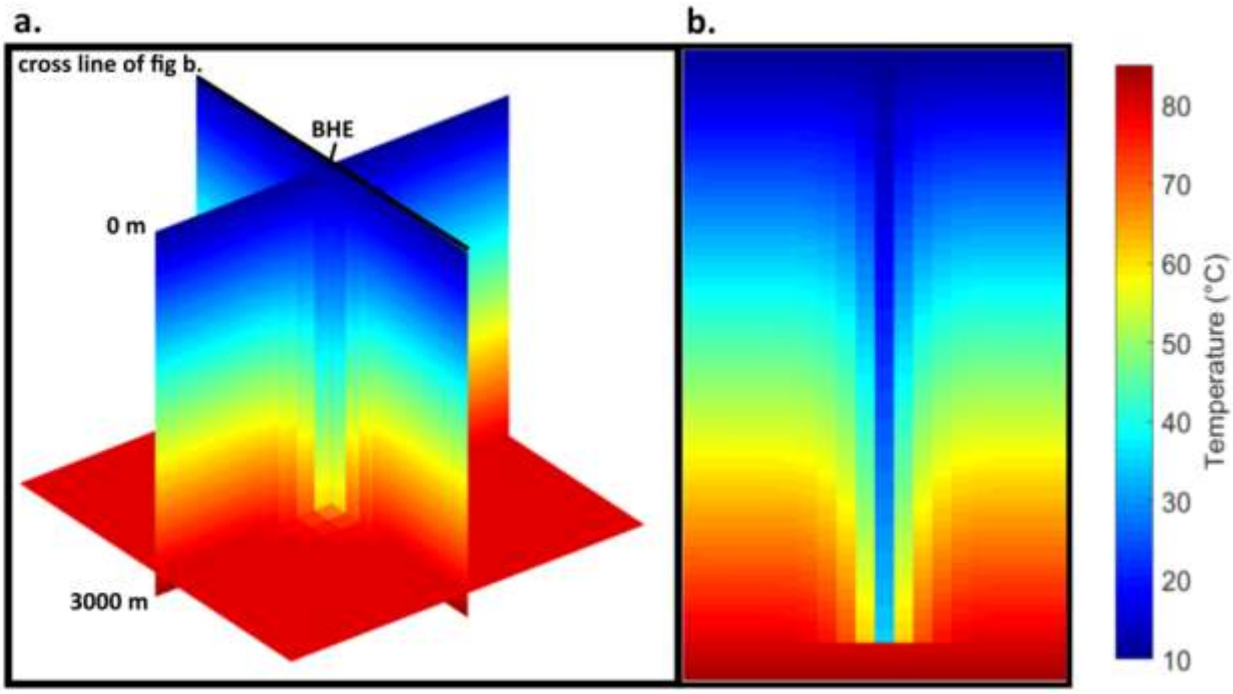

Figure 6. (a) 3D and (b) 2D temperature plots of the subsurface surrounding the borehole heat exchanger after 1 month of continued operation.

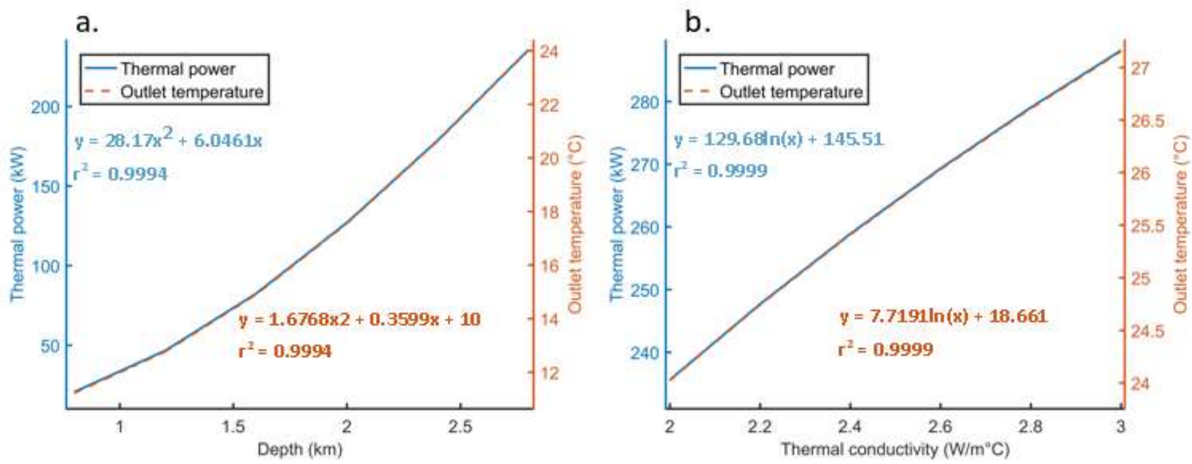

Figure 7. Observed results of the thermal power and outlet temperature for the borehole heat exchanger at the end of the simulation period for varying (a) borehole depths and (b) thermal conductivity of the surrounding rock. The calculated equations for the regression curves are also shown.

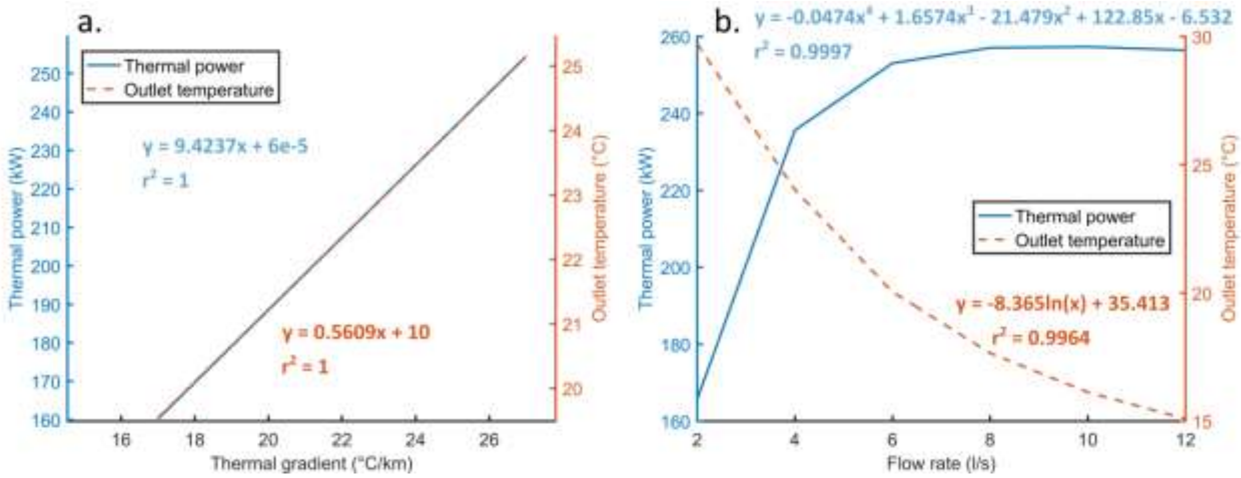

Figure 8. Observed results of the thermal power and outlet temperature for the borehole heat exchanger at the end of the simulation period for varying (a) thermal gradients and (b) flow rates. The calculated equations for the regression curves are also shown.

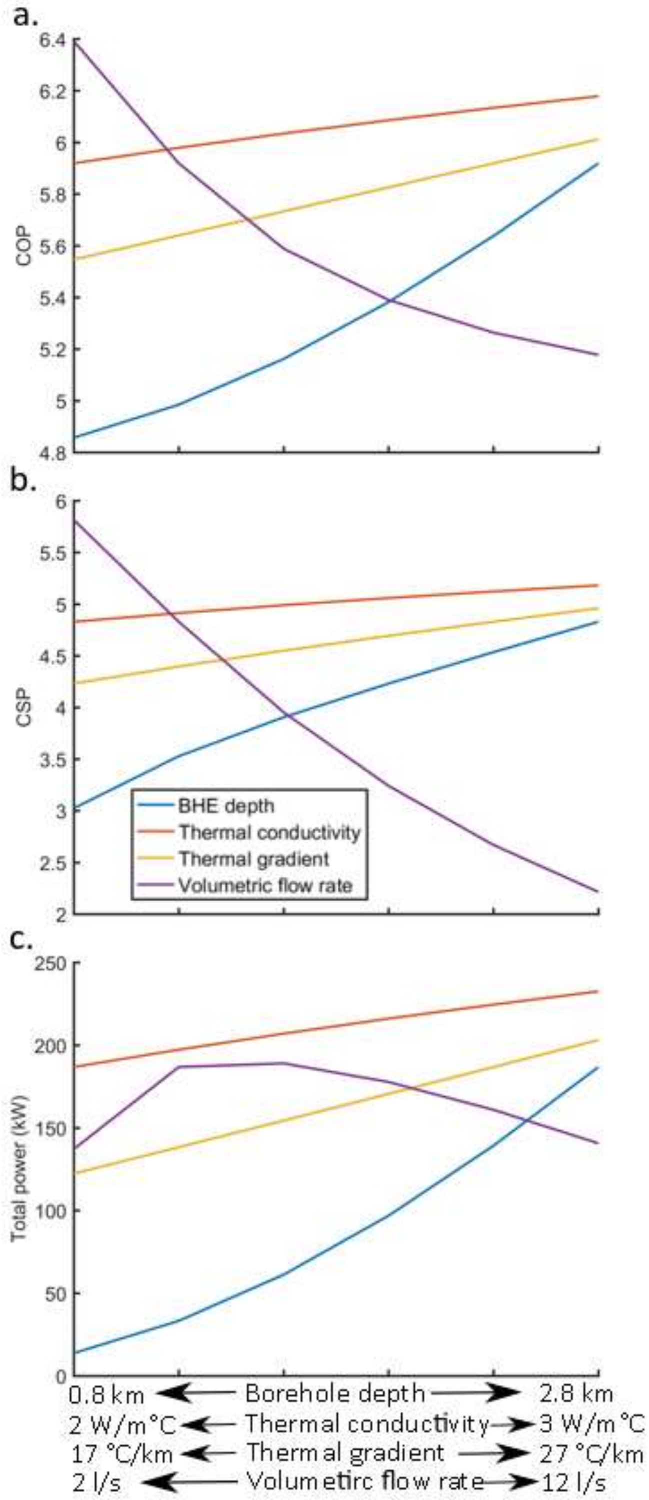

Figure 9. (a) The coefficient of performance (COP) for deep BHEs, (b) coefficient of system performance (CSP) and (c) the total power produced after consideration of parasitic losses in the heat pump and circulation pump. All values measured at the end of the 4 month simulations.

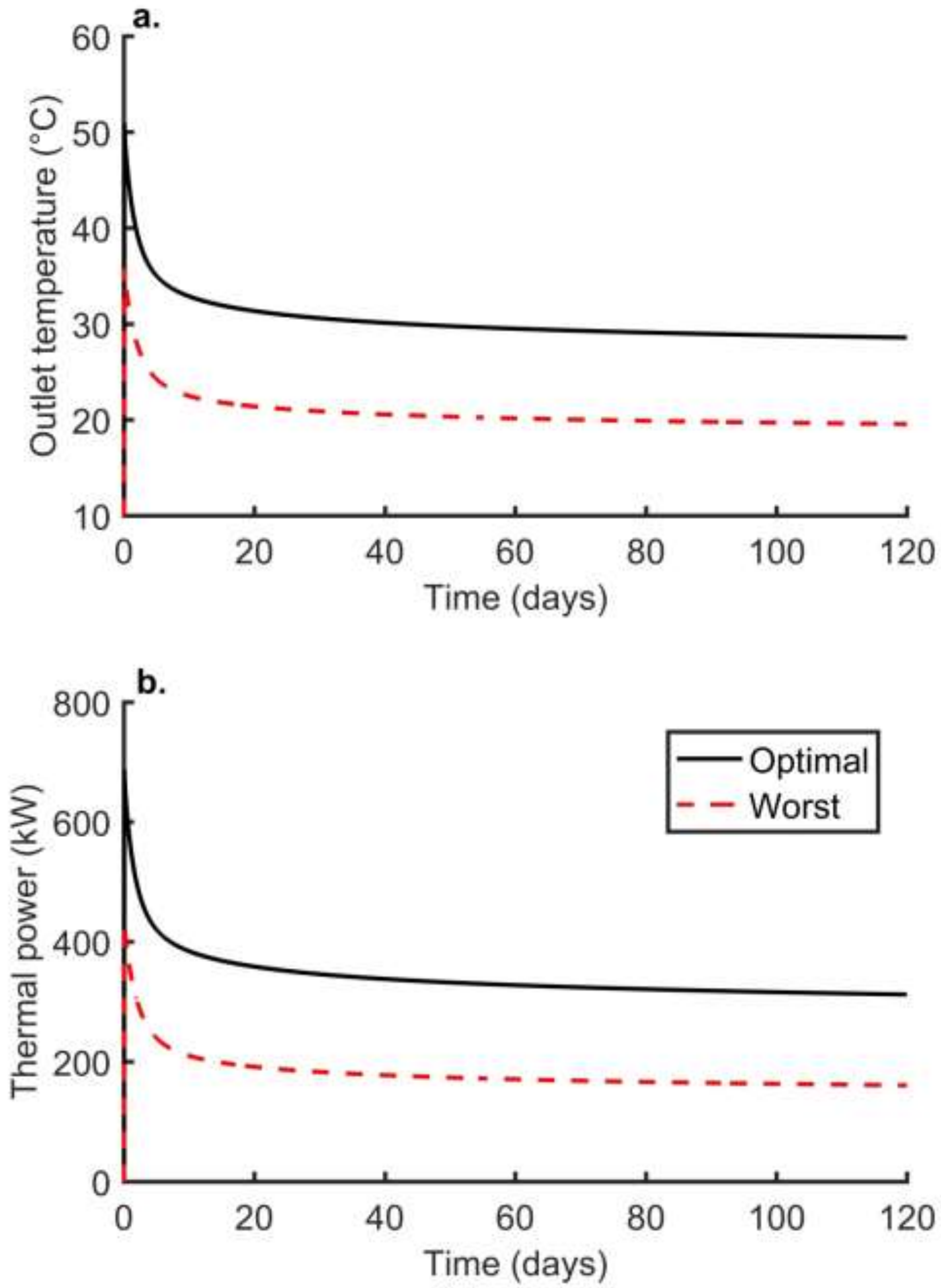

Figure 10. Short term (a) outlet temperature and (b) thermal power plotted against time.

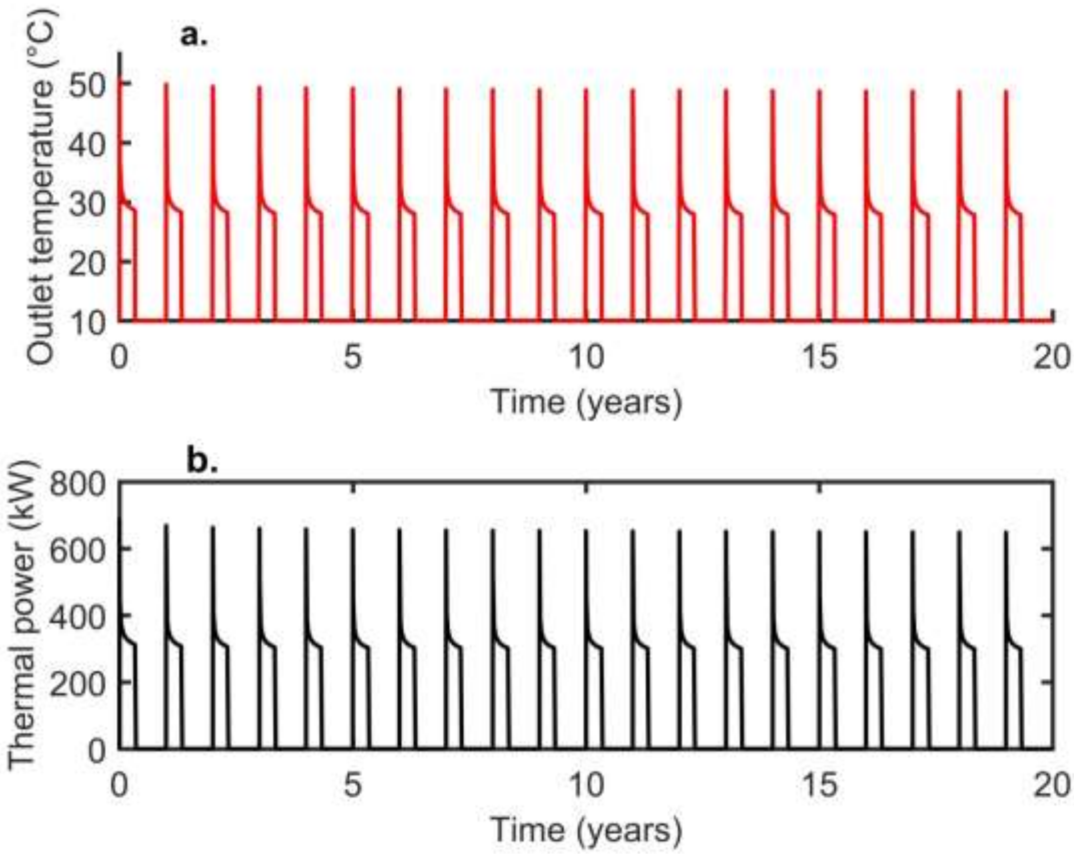

Figure 11. Long term performance analysis showing (a) outlet temperature and (b) thermal power over 20 years for the best case scenario. When the outlet temperature and the thermal power is equal to 10 °C and 0 kW, respectively, the borehole heat exchanger is turned off.

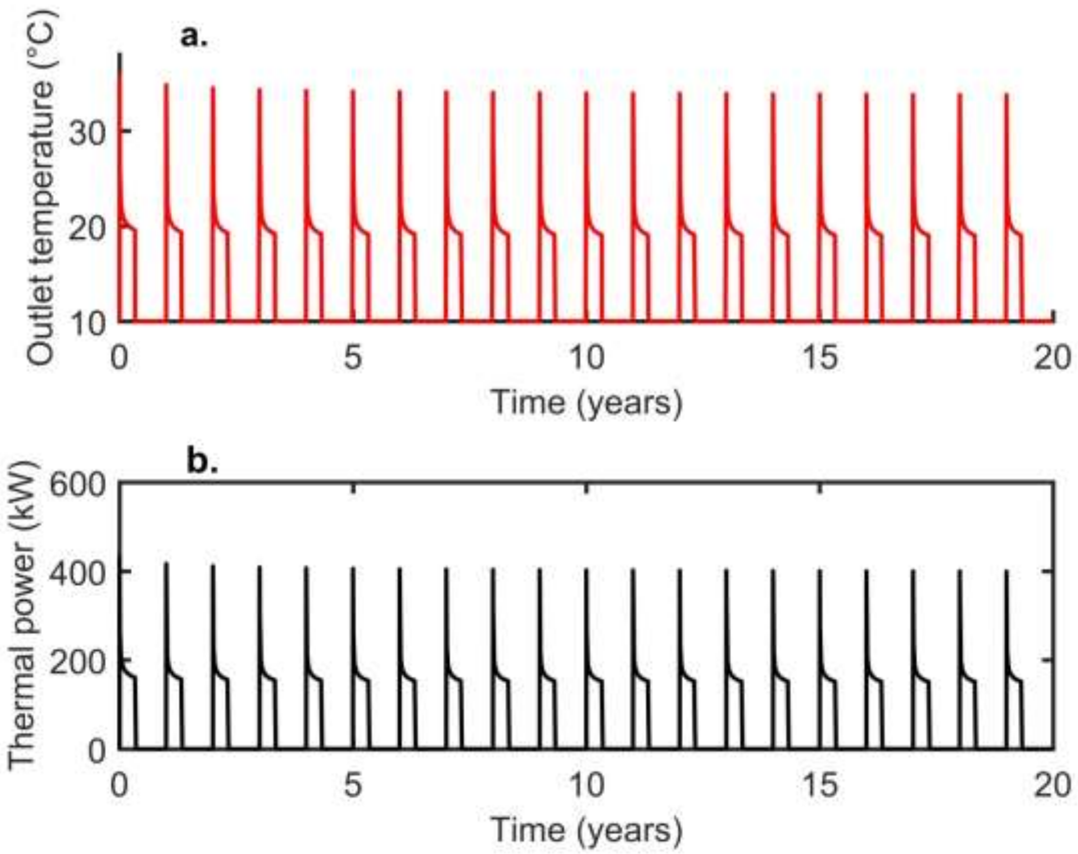

Figure 12. Long term performance analysis showing (a) outlet temperature and (b) thermal power over 20 years for the worst case scenario. When the outlet temperature and the thermal power is equal to 10 °C and 0 kW, respectively, the borehole heat exchanger is turned off.

Parameter	Value	Units	Symbol
Borehole depth	2.8	km	-
Borehole diameter	0.306	m	$2\pi r_{pi}$
Diameter of inner pipe	0.05	m	$2\pi r_{po}$
Thickness of inner pipe	0.01	m	-
Thickness of outer pipe	0.02	m	-
Thickness of grout	0.04	m	-
Thermal conductivity of inner pipe	1	W/m°C	-
Thermal conductivity of outer pipe	45	W/m°C	-
Density of rock	2450	kg/m^3	ρ_s
Thermal conductivity of rock	2	W/m°C	λ_s
Specific heat capacity of rock	775	J/kg°C	C_s
Density of grout	1600	kg/m^3	ρ_g
Thermal conductivity of grout	2.7	W/m°C	λ_g
Specific heat capacity of grout	1250	J/kg°C	C_g
Density of fluid	998	kg/m^3	ρ_f
Thermal conductivity of fluid	0.67	W/m°C	λ_f
Specific heat capacity of fluid	4200	J/kg°C	C_f
Fluid injection temperature	10	°C	-
Surface temperature	10	°C	-
Thermal gradient	25	°C/km	-
Volumetric flow rate	0.004	m^3/s	-

Table 1. Thermo-physical parameters of model.

Parameter	Value	Units
Borehole depth	2.8	km
Average ground temperature	50	°C
Fluid injection temperature	10	°C
Fluid velocity	1	m/s
Density	1000	kg/m^3
Specific heat capacity	4200	J/kg°C
Thermal conductivity	0.67	W/m°C
Thermal resistance	230	W/m^2 °C
Wellbore radius	0.2	m

Table 2. Parameters used in analytical solution.

Parameter	Minimum	Maximum
Borehole depth	0.8 km	2.8 km
Thermal conductivity	2 W/m°C	3 W/m°C
Volumetric flow rate	0.002 m^3/s	0.012 m^3/s
Thermal gradient	17 °C/km	27 °C/km

Table 3. Parameters modelled to test their impact on deep borehole heat exchangers in the Cheshire Basin.